Stamping of a cross-shaped part with 5052, 5754 and 6016 aluminum alloy sheets – experimental and finite element analysis comparison

Rasoul Esmaeilpour, Sobhan Alah Nazari Tiji, Hyunok Kim, Taejoon Park, Hyunki Kim, Farhang Pourboghrat and Bassam Mohammed

December 23, 2018

Stamping of a cross-shaped part with 5052, 5754 and 6016 aluminum alloy sheets – experimental and finite element analysis comparison

R Esmaeilpour[1], S A Nazari Tiji[1], H Kim[1], T Park[1], H Kim[1], F Pourboghrat[1,2], B Mohammed[1,3]

[1] Department of Integrated Systems Engineering, The Ohio State University, 210 Baker Systems, 1971 Neil Avenue, Columbus, OH 43210, United States
[2] Department of Mechanical and Aerospace Engineering, The Ohio State University, 201 W 19th Ave, Columbus, OH 43210, United States
[3] Department of Mechanical Engineering, Michigan State University, 428 S Shaw Ln, East Lansing, MI 48824, United States

Corresponding author e-mail: esmaeilpour.1@osu.edu

Abstract. The application of aluminum alloys is continuing to increase in automotive and aerospace industries. In this study, the stamping of a cross-shaped part, representing typical deep drawn automotive parts, was attempted with three different types of aluminum alloy sheets. To characterize the anisotropic properties of the material, uniaxial tensile tests were performed with ASTM standard dog-bone specimens cut from AA5052, AA5754 and AA6016 T4 alloy sheets. The stamping of the cross-shaped parts was conducted using a high capacity servo press with a servo-cushion system. Deformation strains developing in stamped parts were measured with the ARGUS system for comparison with finite element simulation results. Formed parts were also cut in two different directions using a water-jet machine, and thickness variations along the length of the cut section were measured. The measured surface strains and thickness distributions were compared with finite element simulations results obtained with LS-Dyna explicit code using the Yld2000-2D and Hill's 48 yield functions. Overall, experimental and numerical results correlated well, especially with the Yld2000-2D yield function, implying that this yield function is well suited for the modeling of the complex cross-shaped parts with aluminum alloys.

1. Introduction

Advanced manufacturing technology and weight reduction are two important topics in material processing when it comes to the reduction of energy consumption in transportation industry. Weight reduction can be achieved by optimizing the structural design and usage of lightweight materials, such as magnesium, titanium and aluminum alloys. The application of aluminum alloy, in particular, is increasingly applied in both automotive and aerospace industries. The average usage of aluminum in passenger cars has doubled during the last decade [1-3]. AA6016 is mostly used for the autobody application in Europe. This alloy shows a superior formability and corrosion resistance [1]. Forming behavior of AA6016 was studied by Klos et al. using Hill's 90 yield criterion. They compared cup drawing tests with numerical simulations in order to validate the simulation of complex parts [4]. For fabricating automotive parts like fuel tank, floor panel, side and inner panels, aluminum alloy AA5754 and AA5052 are mostly used [5,6].

Fracture during press forming is a big issue for aluminum alloy sheets because of low ductility. Therefore, optimization of forming conditions to prevent the fracture of aluminum alloy sheets has been widely studied using finite element analysis (FEA). The FEA result accuracy depends on the constitutive model describing the behavior of the material [7]. Many constitutive models have been used to describe the material anisotropy starting with Hill's 48 [8]. During the last three decades, many anisotropic models have been used to improve the modeling of material behavior [9-13]. One of the most famous material models was introduced by Barlat as Yld2000-2D which is an anisotropic yield function for the plane stress condition [14].

In this study, tensile tests for dog bone specimens of three different aluminum alloys, 5052, 5754 and 6016 in 0, 45, and 90 degrees with respect to the rolling direction have been performed. The anisotropic behaviors of these aluminum alloy sheets have been modeled using two different yield functions, Hill's 48 and Yld2000-2D. Then, cross die forming tests were conducted using a high capacity servo press with a servo-cushion system. Strain distribution measurement was performed using ARGUS system based on conventional grid analysis. Cross formed samples were cut using a water-jet machine for thickness measurements in two directions. These experimental results were compared with simulations results using Hill's 48 and Yld2000-2D yield functions in LS-Dyna explicit code.

2. Material characterization

2.1. Uniaxial tensile tests

Uniaxial tests with standard ASTM rectangular dog-bone shaped samples of the three aluminum alloys (AA5052 and AA5754 without any heat treatment and AA6016 with T-4 temper) were performed on a MTS testing machine to obtain the stress-strain curves and anisotropic properties at room temperature. Two extensometers were used to measure the longitudinal and width strain during the test. Tensile coupons were fabricated in three different directions i.e. rolling direction (RD), diagonal direction (DD), and transverse direction (TD) to obtain the anisotropy coefficients (R_0, R_{45}, and R_{90}). The tests were repeated three times for each condition. All the tests were done at a strain rate of $0.006s^{-1}$.

2.2 Hill's 48 and Yld2000-2D anisotropy coefficients

By using the measured R_0, R_{45}, and R_{90}, the anisotropy coefficients for the Hill'48 yield function were calibrated as presented in Table 2. It should be noted that for the calibration of Hill's 1948 yield function, the material parameters for out of plane stress components were assumed to be same as the isotropic von Mises yield function, i.e. L = M = 1.5 [15,16]. In addition, the anisotropy coefficients of Yld2000-2D were calibrated using the normalized yield stress values (i.e. $\sigma_0/\sigma_0 = 1$, σ_{45}/σ_0, and σ_{90}/σ_0), as well as the plastic anisotropy values (i.e. R_0, R_{45}, and R_{90}) as listed in Table3. Note that the yield stress and R-value for the balanced biaxial stress mode were assumed to be 1.0. The measured (or assumed) data used for calibration of the anisotropic coefficients are summarized in Table 1.

Table 1. Normalized measured yield stress and R-values for AA5052, AA5754, and AA6016

Material	σ_0	σ_{45}	σ_{90}	σ_b	R_0	R_{45}	R_{90}	R_b
AA5052	1	0.951	0.931	1	0.896	0.696	0.752	1
AA5754	1	0.965	1.021	1	0.928	0.996	1.094	1
AA6016	1	0.973	0.969	1	1.240	0.720	1.150	1

Table 2. Hill's48 anisotropy coefficients for AA5052, AA5754, and AA6016

Material	F	G	H	L	M	N
AA5052	0.6282	0.5275	0.4725	1.5	1.5	1.3816
AA5754	0.4401	0.5185	0.4815	1.5	1.5	1.4345
AA6016	0.4814	0.4464	0.5536	1.5	1.5	1.1319

Table 3. Yld2000-2D anisotropy coefficients for AA5052, AA5754, and AA6016

Material	α_1	α_2	α_3	α_4	α_5	α_6	α_7	α_8
AA5052	0.934	1.092	0.870	1.044	1.012	1.013	1.009	1.169
AA5754	1.001	0.981	1.041	0.988	1.000	0.983	1.030	1.084
AA6016	0.980	1.072	0.967	1.008	0.997	1.022	0.995	1.109

3. Cross die forming process

The cross die forming test was conducted using a 300-Ton AIDA servo press with a 25-Ton servo-cushion system. The punch speed was set at 15 stroke per minute (SPM), and a blank holder force of 50 KN were used. In the cross die forming test, the orientation of the blank can be changed to produce different forming behavior. Figure 1 shows the rolling direction (RD) of the blank, which is along the cross. Cross die forming test specimens are 470 mm x 470-mm rectangular sheets with thicknesses of 1mm for AA5052, 0.9mm for AA5754, and 1.2mm for AA6016. A stamping lubricant was applied on the both sides of the blank using the UNIST Motorized Roller System. The etched grid pattern was applied on each sample before the forming processes, and the strain distributions were measured by the grid analysis in ARGUS system, in which the strain values were calculated by comparing before and after grid shapes.

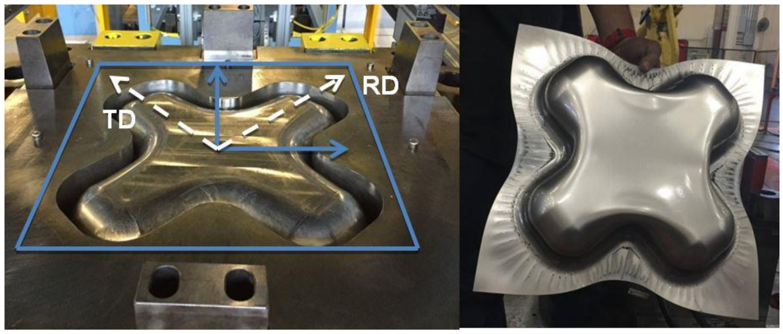

Figure 1. Schematic of Specimen Orientations and a Sample Cross Formed Part

Experimental results from the cross die forming tests were compared with the simulations result performed in LS Dyna explicit code using two anisotropic yield functions i.e. Hill's 48 and Yld2000-2D. It should be noted that for this study, Swift type hardening model was primarily selected over other types of hardening laws (e.g., Voce) because it exhibited the hardening behavior of the current material accurately. As for the simulations, element size of 5mm and a total number of 8836 quadrilateral shell elements were used for the blank. The blank was only constrained by friction in the analysis with no additional boundary conditions. The blank was placed between a blank-holder and a die. The blank-holder force was 50 KN. The punch was considered stationary, while the die moved toward the punch by 96 mm depth with a velocity of 300 mm/s. The friction coefficient of 0.15 was assumed. The thinning of the sheet is one of the most important factors to be considered in the sheet metal forming process. Figures 2-4 shows the thinning of Al5052 in depth of 90 mm, Al5057 in depth of 83 mm, and Al6016 in depth of 71 mm as the formability of these aluminum alloys are different. The contours for the experimental measurement and simulation results with Yld2000-2D are almost identical, which means this model is a better representative of the material behavior. It should be noted that the thinning measurement was not captured at the wall areas due to the removal of etched patterns of the aluminum surface. In Figure 5 cross formed samples were cut along two orientations i.e. along the cross and 45 degrees to the cross using a water-jet machining for thickness measurements which was done at 15mm intervals. The same procedure was performed in the simulations, in order to measure the thickness reduction of the deformed samples along the same orientations.

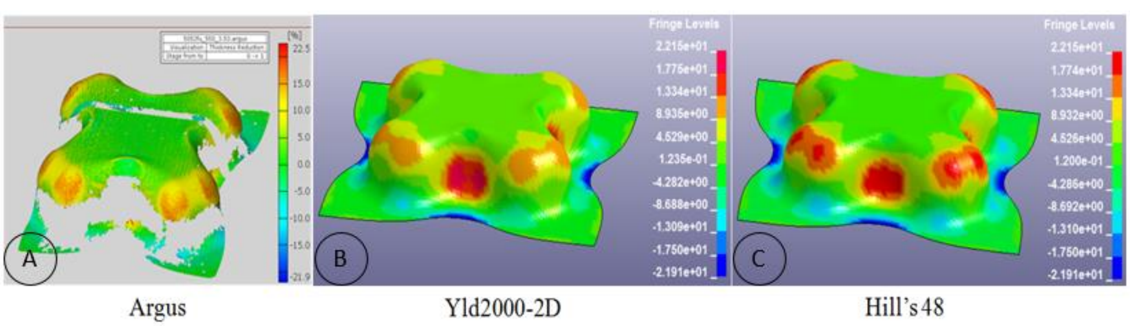

Figure 2. AA5052 thinning distribution contours: A) experimental measurement using Argus, B) FEM simulation results by using Yld2000-2D, C)FEM simulation results by using Hill's.

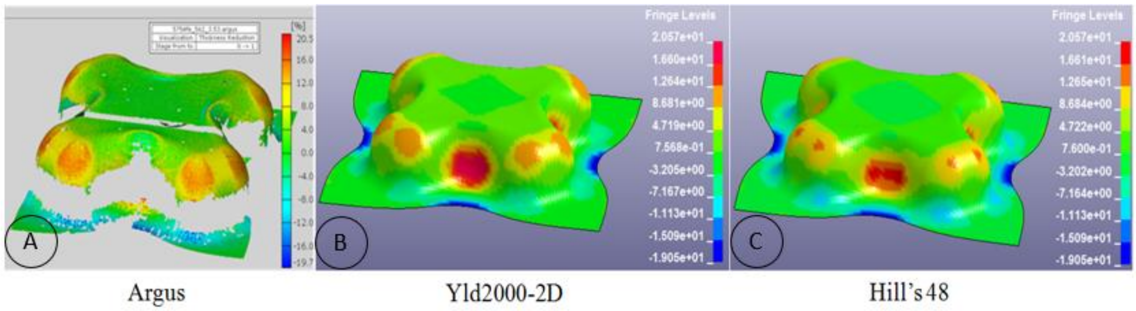

Figure 3. AA5754 thinning distribution contours: A) experimental measurement using Argus, B) FEM simulation results by using Yld2000-2D, C) FEM simulation results by using Hill's

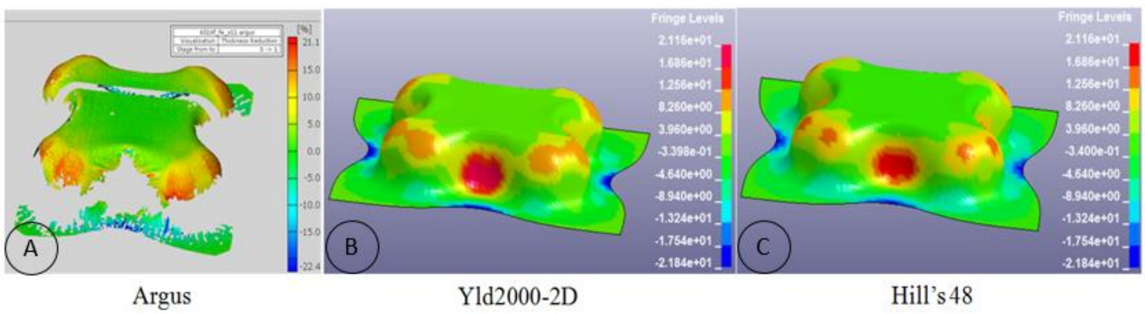

Figure 4. AA6016 thinning distribution contours: A) experimental measurement using Argus, B) FEM simulation results by using Yld2000-2D, C) FEM simulation results by using Hill's

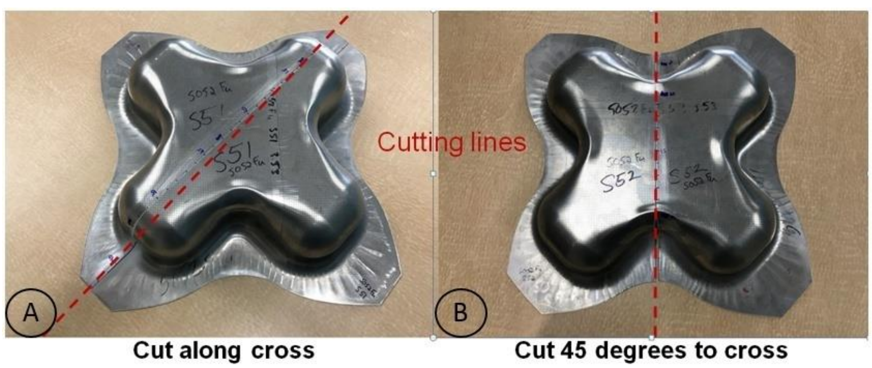

Figure 5. samples cut orientations for thickness measurements: A) along cross, B) 45 degrees to cross

5. Conclusions

This study showed that Yld2000-2D and even Hill's 48 are decent representative of anisotropy behavior of aluminum alloys namely; AA5052, AA5754 and AA6016 T-4 in the cross forming process. As for material characterization, uniaxial tensile tests of AA5052, AA5754 and AA6016 T-4 dog-bone specimen were performed to obtain the stress-strain curves and the anisotropic properties. Since a two-dimensional (2D) plane stress yield function is sufficient to capture the mechanical behavior in conventional metal forming processes, such as stamping, Yld2000-2D and Hill's 48 yield functions anisotropy coefficients were calibrated to predict the anisotropic properties of these aluminum sheets. Compared to Hill's 48, Yld2000-2D showed better prediction of the anisotropy (for both R-value and yield stress distribution). These two yield functions were used to simulate the cross die forming process in LS-Dyna explicit code and compared with the experiments conducted using a high capacity servo press with servo-cushion system. Furthermore, the thinning and strain distribution of the cross formed blanks obtained from FEM analysis were compared with the measured values obtained through ARGUS grid analysis. The simulation results and the experiments were almost identical especially with the Yld2000-2D.

Acknowledgement
This study was supported by EWI's Joint Industry Project (JIP) sponsors and the Ohio Development Service Agency (ODSA) on Advanced Manufacturing Program (AMP 15-08). The authors would like to thank the Forming Center of EWI for the support given to this research.

References

[1] Hirsch J 2017 Recent development in aluminium for automotive applications *Trans. Nonferrous Met. Soc. China* **24** 1995–2002

[2] Asgharzadeh A, Jamshidi Aval H and Serajzadeh S 2016 A Study on Flow Behavior of AA5086 Over a Wide Range of Temperatures *J. Mater. Eng. Perform.* **25** 1076–84

[3] Ebrahimi M, Djavanroodi F, Tiji S, Gholipour H and Gode C 2015 Experimental Investigation of the Equal Channel Forward Extrusion Process *Metals (Basel).* **5** 471–83

[4] Klos A, Kahrimanidis A, Wortberg D and Merklein M 2017 Experimental and numerical studies on the forming behavior of high strain Al-Mg-Si (-Cu) sheet alloys *Procedia Eng.* **183** 95–100

[5] Kesharwani R K, Basak S, Panda S K and Pal S K 2017 Improvement in limiting drawing ratio of aluminum tailored friction stir welded blanks using modified conical tractrix die *J. Manuf. Process.* **28** 137–55

[6] Garware M, Kridli G T, Mallick P K, Garware M, Kridli G T, Mallick P K and Materials L A 2010 Tensile and Fatigue Behavior of Friction-Stir Welded Tailor-Welded Blank of Aluminum Alloy 5754 **19** 1161–71

[7] Laboratories A 1992 Finite element simulation of sheet metal forming for planar anisotropic metals **8** 453–76

[8] Hill R. A theory of the yielding and plastic flow of anisotropic metals. *Proc. Roy. Soc.* 1948;**193**, 281–297.

[9] Hill R 1987 CONSTITUTIVE DUAL POTENTIALS IN CLASSICAL PLASTICITY t / J (q) t / J (q) **35** 23–33

[10] Met J and Britain G 1993 A GENERAL YIELD CRITERTON USING BOUNDS AND A TRANSFORMATION WEIGHTING **41** 1859–86

[11] Bron F and Besson J 2004 A yield function for anisotropic materials Application to aluminum alloys **20** 937–63

[12] Esmaeilpour R, Kim H, Park T, Pourboghrat F and Mohammed B 2017 International Journal of Mechanical Sciences Comparison of 3D yield functions for finite element simulation of single point incremental forming (SPIF) of aluminum 7075 *Int. J. Mech. Sci.* **133** 544–54

[13] Esmaeilpour R, Kim H, Park T, Pourboghrat F, Xu Z, Mohammed B and Abu-Farha F 2018 Calibration of Barlat Yld2004-18P Yield Function Using CPFEM and 3D RVE for the Simulation of Single Point Incremental Forming (SPIF) of 7075-O Aluminum Sheet *Int. J. Mech. Sci.* **145** 24–41

[14] Barlat F, Brem J C, Yoon J W, Chung K and Dick R E 2003 Plane stress yield function for aluminum alloy sheets — part 1 : theory **19** 1297–319

[15] Mohammed B, Park T, Pourboghrat F, Hu J, Esmaeilpour R and Abu-farha F 2017 strength steel **0** 1–19

[16] Mohammed B, Park T, Kim H, Pourboghrat F and Esmaeilpour R 2018 The forming limit curve for multiphase advanced high strength steels based on crystal plasticity finite element modeling *Mater. Sci. Eng. A* **725** 250–66